Supplementary Figure legends

Supplementary Figure 1: Long term follow up of changing hair cycle domains on dorsal skin of the same mouse.
The same *Msx2* null mouse[9] was followed for over 145 days to trace the temporal changes of hair cycle domains. Pictures were taken every 2-3 days and selective ones are shown here. In normal pigmented mice, similar hair cycle domains can be revealed by simple hair clipping. This is possible because the skin of pigmented mice produce pigments only in anagen hair follicles, starting from anagen III and onwards.

Supplementary Figure 2: Defining competence and refractory phases by hair plucking.
Early or late telogen skin regions were chosen as described in supplementary methods (region c). To help observe the emergence of new hair filaments, the hair in a larger area is clipped close to the skin surface (region b). The designated number of hairs are then plucked from the central region (region a). Note the other (clipped but non-plucked) hairs in region b are still in telogen. Because in pigmented mice the proximal part of a mature telogen club hair filament is virtually non-pigmented, such closely clipped club hairs in region b often appear nearly transparent / white. When 50 or 200 hairs were plucked, regrown hairs do not appear at once, but rather within about a 24 hour interval. To make the picture clearer, photos shown represent hair filaments that have continued to grow for several days.

Hair regeneration in the plucked region (arrowhead) is shown by the pigmented hairs, or "+" in some panels. The more hairs are plucked, the earlier anagen starts. Plucking stimulated hair regeneration was initially described in Collins, H.H. Studies of normal moult and artificially induced regeneration of pelage in Peromyscus. *J. Exp. Zool.* **27,** 73–95 (1918).

Supplementary Figure 3: Spatial and temporal changes of *Bmp4-lacZ* expression in the regenerating hair wave.
Bmp4-lacZ transgenic mice were used to show *Bmp4* expression (Kulessa, H., Turk, G., Hogan, B.L. Inhibition of Bmp signaling affects growth and differentiation in the anagen hair follicle. *EMBO J.* **19,** 6664-74 (2000)). View of a skin strip showing *Bmp4-lacZ* activity (blue) in refractory telogen and an absence of activity in competent telogen. The high power views in the two lower rows show *Bmp4-lacZ* activity to be first expressed intra- and inter-follicularly, then limited to the follicle, and eventually to disappear. *Bmp4-lacZ* activity is regained during anagen. Activity is seen in the dermal papilla and secondary hair germ during anagen initiation. Later it also appears in the outer root sheath.

E – epidermis; Inf – infundibulum; SG – sebaceous gland; ORS – outer root sheath; Germ – secondary hair germ; DP – dermal papilla, DF – dermal fibroblasts; Muscle – arrector pili muscle. Scale bars: 1 mm and 200 um and 50 um.

Supplementary Figure 4: Spatial and temporal changes of *NOG-lacZ* expression in the regenerating hair wave.
A longitudinal skin strip from *NOG-lacZ* mice (Brunet, L.J., McMahon, J.A., McMahon, A.P., Harland, R.M. Noggin, cartilage morphogenesis, and joint formation in the mammalian skeleton. *Science.* **280,** 1455-7 (1998)). Wave front and boundary regions are marked. Blue, X-gal staining; black, melanin. The stepwise high power view transgene expression in the follicles throughout the hair cycle. Mesenchymal transgene expression occurs only during anagen: first in the dermal sheath and later in the dermal papilla and basal stalk.

DP – dermal papilla; DS – dermal sheath; Matrix – epithelial matrix of the hair follicle; Stalk – basal stalk.
Scale bars: 5 mm and 200 um.

Supplementary Figure 5: Spatial and temporal changes of *Bmp2* expression in the regenerating hair wave.
(a-e) Dynamic expression of *Bmp2* in a strip of skin containing a propagating hair cycle domain. The dark field illumination is used to highlight the contrast.
(a) Different hair cycle stages are spread spatially on a longitudinal skin strip. *In situ* hybridization for *Bmp2*. Blank arrows, the direction of the spreading waves; --| sign, boundary between anagen (An, which was competent telogen) and refractory telogen (Refr. Tel). Two boxed regions showing the wave front and boundary are enlarged in panel (b) and (c). Also note the change of skin thickness.
(b, c) *Bmp2* is negative in the wave front region which includes competent telogen and propagating anagen. Inter-follicular *Bmp2* starts to appear around anagen IV and its expression becomes stronger in anagen VI (yellow arrows). Inter-follicular *Bmp2* persists into the refractory telogen stage (red arrows).
(d) Progressive changes of panel (c). Entering late telogen, the region right of the boundary becomes *Bmp2*-negative (green arrows) and competent to enter anagen. However, anagen VI (yellow arrow) follicles are not able to induce these competent telogen follicles and the boundary remains stable.
(e) A telogen skin strip shows *Bmp2* expression during early and refractory phases (red arrows), but lack thereof during late and competent phase (green arrows).
(f) Intra-follicular (black arrow) and inter-follicular *Bmp2* expression (red arrow) can be seen more clearly on whole mount samples from albino mice.
(g) A long skin strip spanning two hair cycle domains shows two *Bmp2*-expressing segments. (h) Double staining with Sudan red (red) shows transcripts are present in some adipocytes (i, i') High power view of inter-follicular *Bmp2* expression. Blue color – *in situ* staining. *Bmp2* transcripts are clearly located in inter-follicular cells.

Scale bars: a: 1 mm; b-e: 500 um; f,: 200um and 100um; h: 200 um; i, i': 100 um.

Supplementary Figure 6: Changes in pSMAD expression during hair cycling.
(a) pSMAD immuno-staining is present in follicular epithelium, including bulge area (insert) and adjoining infundibulum (green arrow).

(b) Since skin in its second telogen phase (45-70 day after birth) is usually used in hair follicle and carcinogenesis studies, we show results at this stage, which are consistent with older mice.

Supplementary Figure 7: Interactions of small *KRT14-NOG* skin transplant with the host skin macro-environment. When a small graft of *KRT14-NOG* skin (~1mm in diameter) was transplanted, the donor skin remained in telogen longer (a) and could respond to an anagen activating wave originating from the host (b). Thus we achieved partial functional rescue of *KRT14-NOG* phenotypes. On some occasions, some grafts exhibited a greater degree of autonomous control (c) and can induce host hair follicles surrounding the perimeter of *KRT14-NOG* skin graft into anagen (d). Pigmented hairs are from donor *KRT14-NOG.* White hairs are from SCID mice.

Supplementary Figure 8: BMP protein can convert competent telogen status to refractory.
(a) hBMP4-soaked beads caused hair propagation wave (green arrowed curve) to go around them, creating a new telogen domain. (b) Albumin does not have this effect. Red broken line, domain border.

Scale bars: 1 mm.

Supplementary Figure 9: Cyclic molecules expression during hair cycling.
In a strip of skin, cyclic TOPGAL-lacZ reporter activity (DasGupta, R and Fuchs, E. Multiple roles for activated LEF/TCF transcription complexes during hair follicle development and differentiation. *Development* **126:** 4557-4568 (1999)) and *Msx2* expression are in phase with the hair cycle rhythm.

Scale bars: 1mm and 200 um.

Supplementary Figure 10: Schematic summary of multiple expression sites of *noggin*, *Bmp4* and *Bmp2* during functional phases of the hair cycle.

Supplement References

1. Oh, H.S. and Smart, R.C. An estrogen receptor pathway regulates the telogen-anagen hair follicle transition and influences epidermal cell proliferation. *PNAS.* **93:** 12525-30 (1996).

2. Craven, A.J., Nixon, A.J., Ashby, M.G., Ormandy, C.J., Blazek, K., Wilkins, R.J., Pearson, A.J. Prolactin delays hair regrowth in mice. *J Endocrinol.* **191:** 415-25 (2006).

Supplementary Figure 1

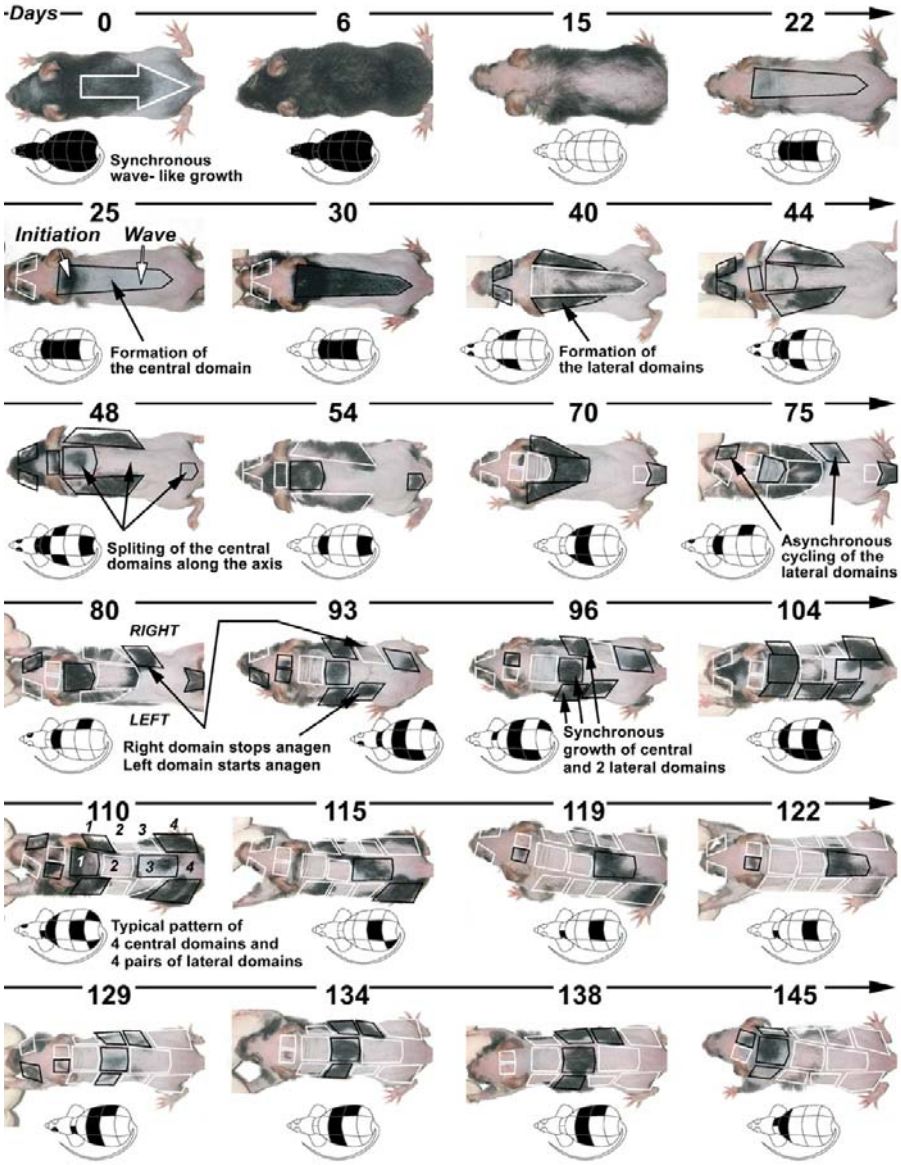

Supplementary Figure 2

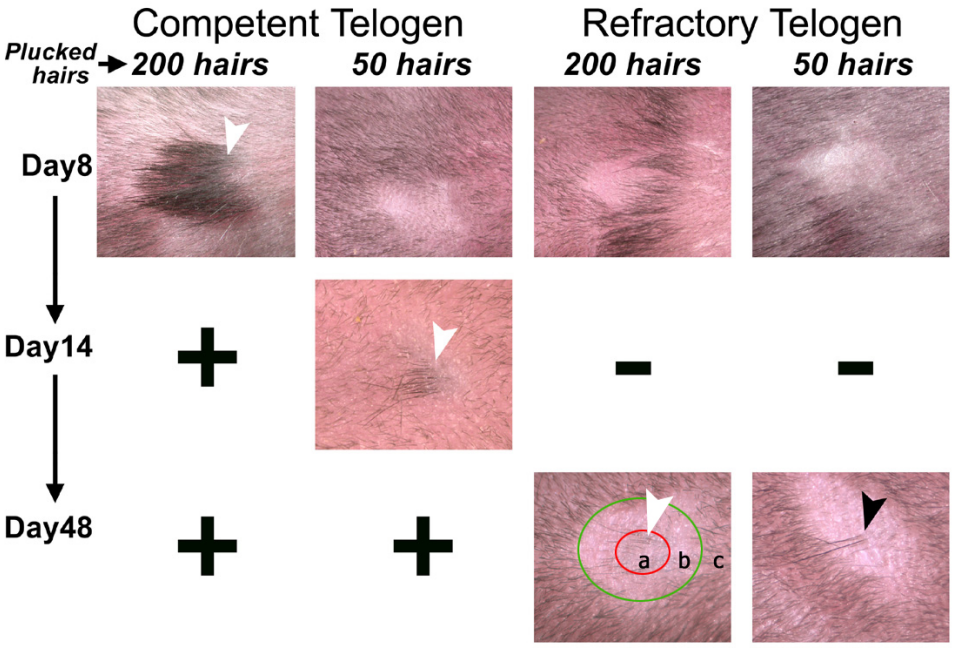

Supplementary Figure 3

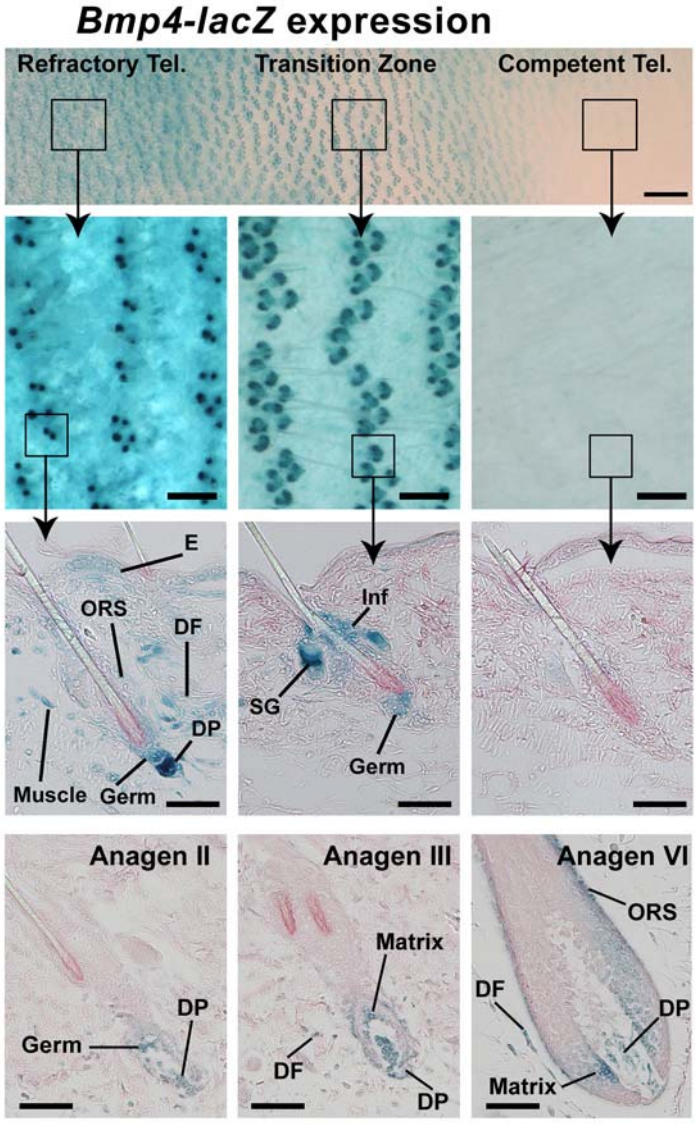

Supplementary Figure 4

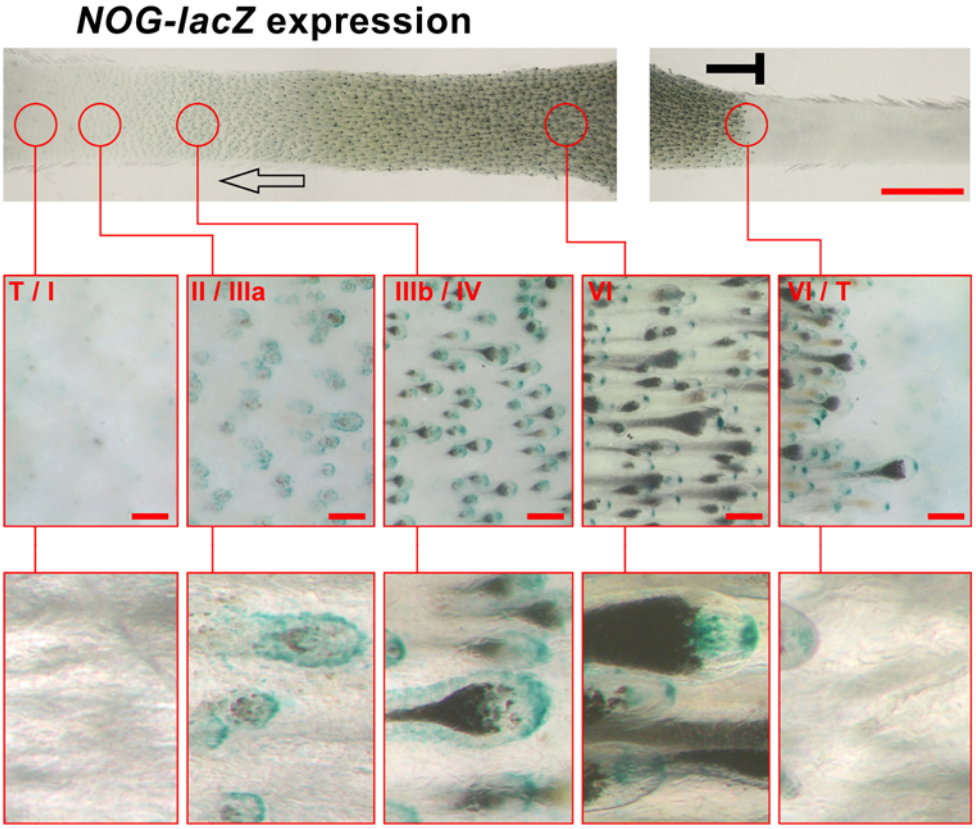

Supplementary Figure 5

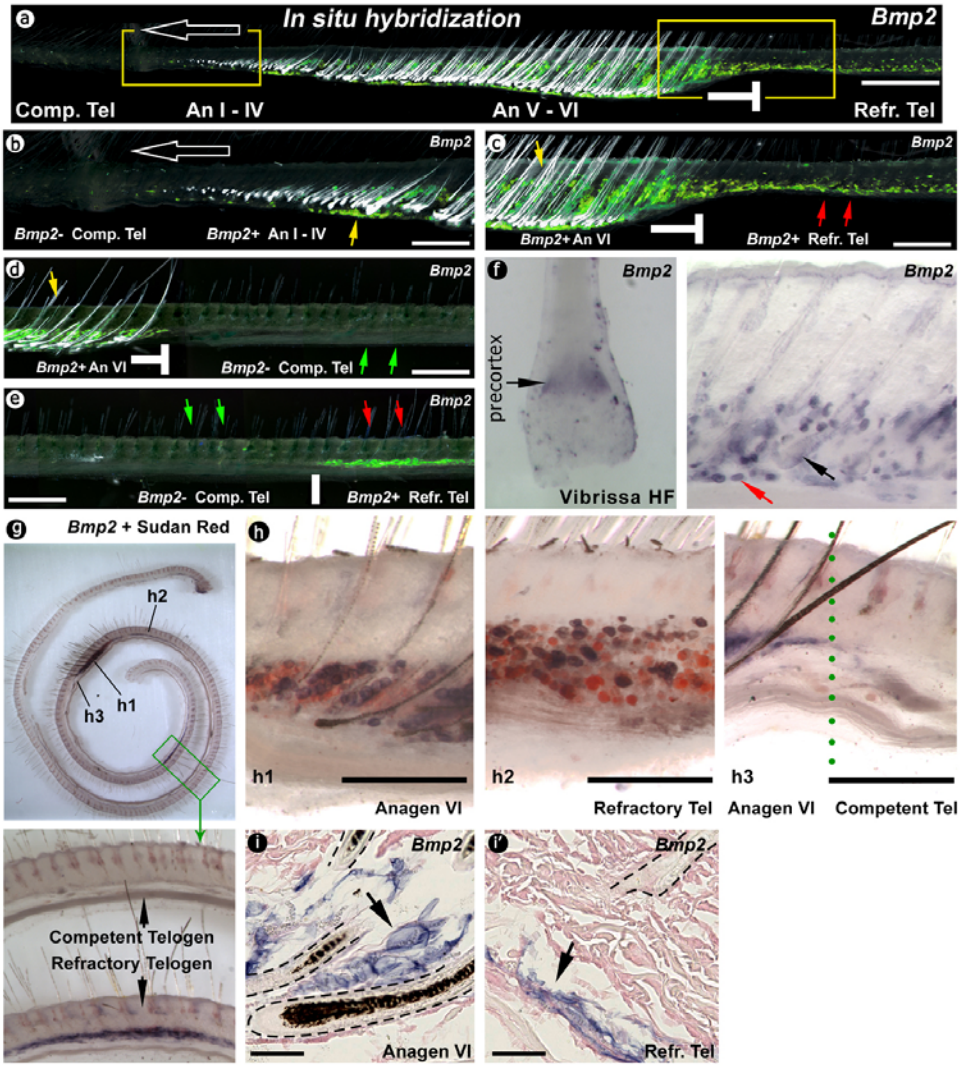

Supplementary Figure 6

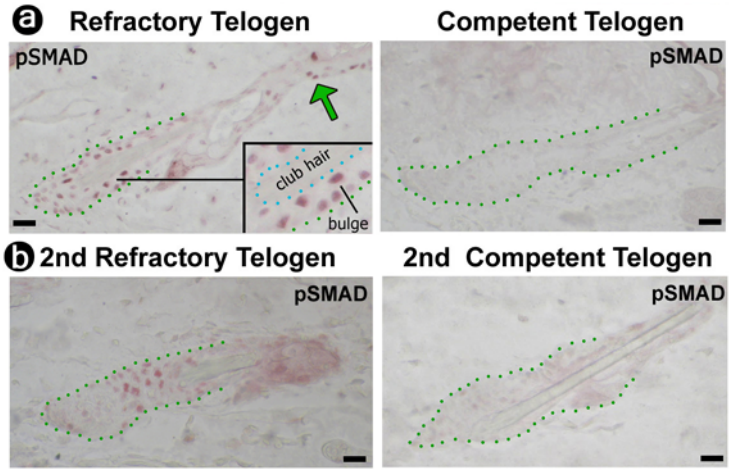

Supplementary Figure 7

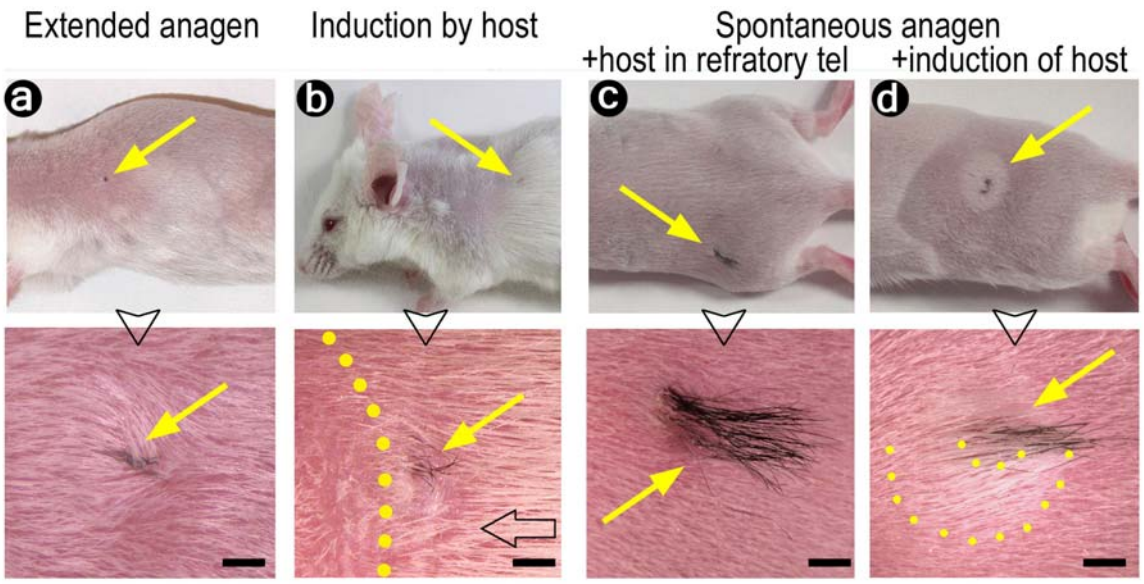

Supplementary Figure 8

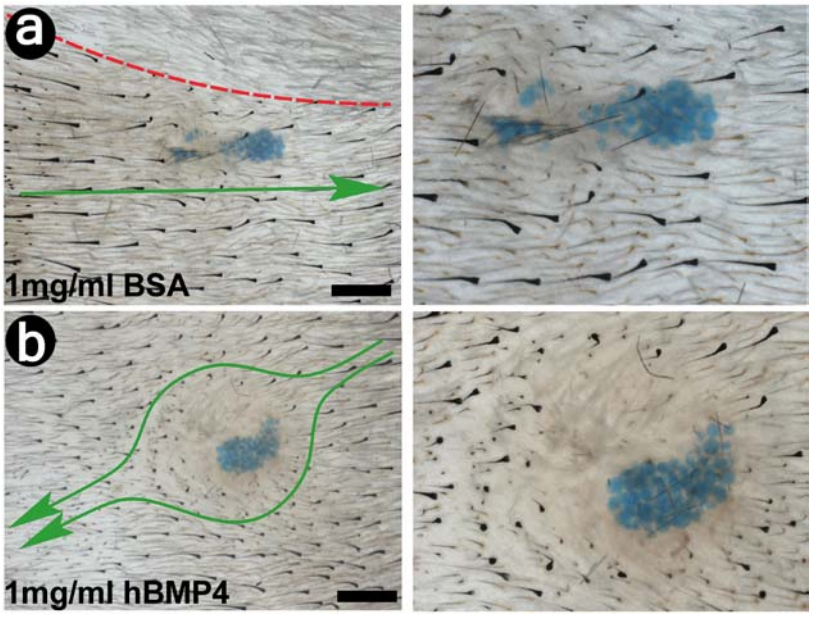

Supplementary Figure 9

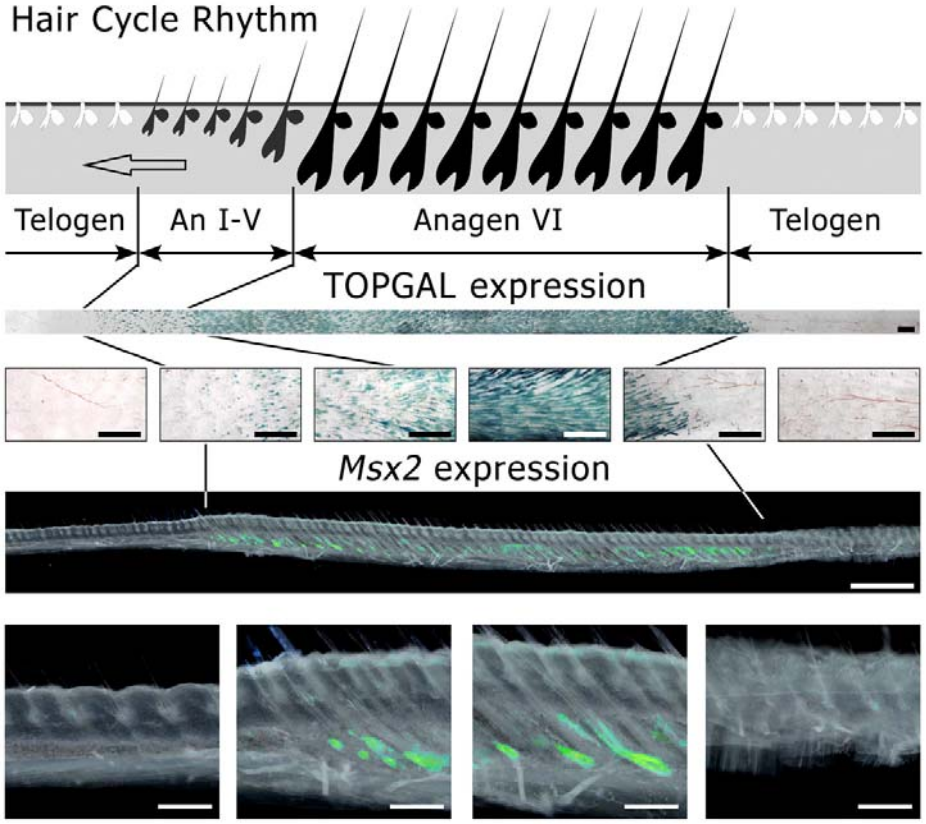
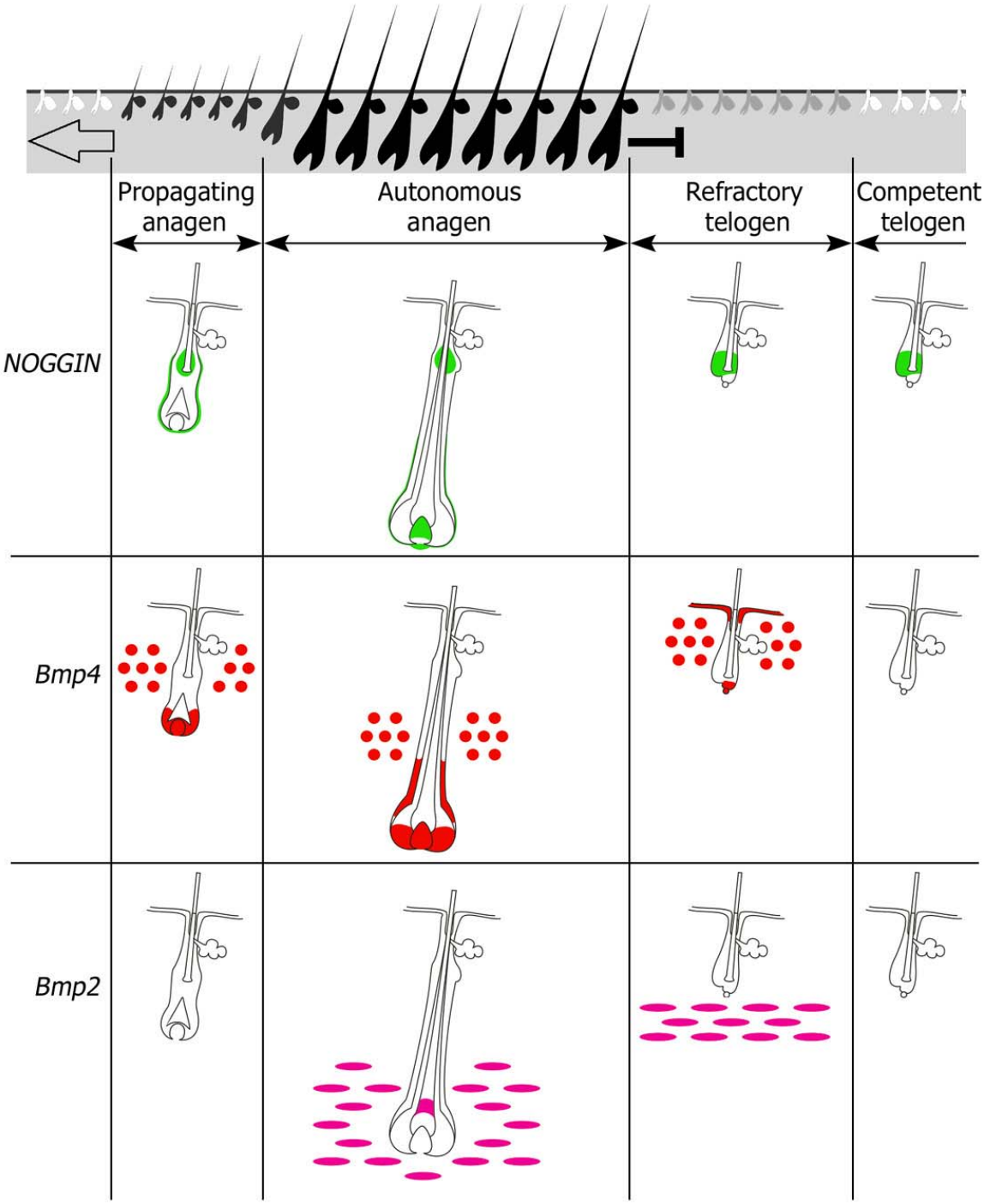
Supplementary Figure 10